ISSN 2075-1133, Inorganic Materials: Applied Research, 2024, Vol. 15, No. 3, pp. 626–635. © Pleiades Publishing, Ltd., 2024.
Russian Text © The Author(s), 2023, published in Fizika i Khimiya Obrabotki Materialov, 2023, No. 5, pp. 5–17.

EFFECTS OF ENERGY FLUXES ON MATERIALS

Thermal Stability of the Structural and Phase State of Aluminum and Alloys of the Al–Si System Doped with Zirconium Atoms under the Influence of Compression Plasma Flows

N. N. Cherenda[a], *, N. V. Bibik[a], V. M. Astashynski[b], and A. M. Kuzmitski[b]

[a] *Belarusian State University, Minsk, 220030 Belarus*

[b] *Lykov Heat and Mass Transfer Institute, National Academy of Sciences of Belarus, Minsk, 220072 Belarus*

**e-mail: cherenda@bsu.by*

Received September 26, 2022; revised November 22, 2022; accepted December 20, 2022

Abstract—The structural and phase state of the surface layers of Al, Al-Si, and Al-Si-Cu-Mg alloys doped with zirconium atoms under the influence of compression plasma flows is studied. It is established that metastable compounds Al_3Zr with the crystal structure $L1_2$ and $(Al, Si)_3Zr$ with the structure $D0_{22}$ are formed in the doped layers of aluminum and silumins, respectively. It is shown that doping of the studied alloys with zirconium makes it possible to increase the microhardness of the surface layer by 1.4–3 times. A study of the thermal stability of the structural and phase state of the doped layers at 550°C showed that, as a result of aluminum annealing, the Al_3Zr phase with the $L1_2$ structure transforms into the Al_3Zr compound with the $D0_{23}$ structure, and in the alloys of the Al–Si system, the decomposition of $(Al,Si)_3Zr$ and the formation of $ZrSi_2$ occur. It is noted that the synthesized surface layer has increased temperature strength.

Keywords: silumin, aluminum, zirconium, compression plasma flows, doping, annealing, phase and elemental composition, microstructure, microhardness

DOI: 10.1134/S2075113324700059

INTRODUCTION

A separate group of casting Al–Si alloys consists of piston complex alloyed silumins, the physical and mechanical properties of which are subject to such requirements as low coefficient of thermal expansion, high thermal conductivity, and high heat resistance. One of the most widely used piston eutectic silumins is the Al-Si-Cu-Mg alloy, which contains copper, magnesium, nickel, and other doping elements. However, the use of eutectic piston silumins, in particular, for the manufacture of heavily loaded and forced engines, is limited by their insufficiently high-temperature strength [1].

As shown in [2–7], the treatment of silumins with high-energy energy flows makes it possible to modify the mechanical properties of the surface layers of these alloys. Therefore, doping with zirconium atoms under conditions of nonequilibrium crystallization, which ensures the formation of a supersaturated solid solution and the formation of strengthening high-temperature intermetallic compounds, is one of the promising ways to increase the thermal stability and strength characteristics of aluminum alloys [8, 9]. It is known that, under conditions of equilibrium crystallization of aluminum alloys at a low concentration of zirconium, an Al_3Zr phase with a tetragonal structure $D0_{23}$ is formed, which has needle-like precipitates and is undesirable in the structure since it worsens the plastic properties. However, an increase in the cooling rate makes it possible to form a supersaturated Al(Zr) solution that decomposes into dispersed Al_3Zr inclusions with a cubic $L1_2$ structure, which increase the recrystallization temperature of the alloy [10, 11]. It should be noted that the presence of silicon in the alloy composition can lead to the appearance of the $(Al,Si)_3Zr$ phase with the $D0_{22}$ structure designated in the literature as τ_1 [12–15], which is not characteristic of the equilibrium Al–Zr binary system and differs from the Al_3Zr phase with $D0_{23}$ in a reduced crystal lattice parameter c. To date, this phase is poorly studied since there is insufficient data on its thermal stability and influence on the physical and mechanical properties of silumins.

Ultrafast cooling conditions can be achieved with doping of the surface layer of metals and alloys by applying a coating containing zirconium and by subsequent treatment with high-energy particle flows that ensure melting of the coating–substrate surface layer and liquid-phase mixing of the melt components. The use of compression plasma flows (CPFs) for these purposes in earlier studies on the doping of various

metals and semiconductors has shown its prospects [16–18]. Impact of plasma pulses leads to melting of the surface layer, mixing of the coating–substrate system, and subsequent crystallization under ultrafast cooling conditions (~10^5–10^7 K/s).

The aim of the study is to investigate the structural and phase state of the near-surface composite layer formed by doping of aluminum and alloys of the Al–Si system with zirconium atoms under the influence of compression plasma flows, as well as the thermal stability of the synthesized zirconium trialuminides and the microhardness of the near-surface doped layer before and after annealing at 550°C.

EXPERIMENTAL

The objects of study were pure aluminum, silumin Al-Si (12.6 at % Si, 0.1 at % Fe), and Al-Si-Cu-Mg alloy containing (in at %) 12.6 Si, 0.5 Cu, 2.7 Mg, 0.3 Ni, 0.3 Fe, and 0.2 Mn. The samples were made in the form of cylinders with a diameter of 15 mm and a height of 5 mm.

A zirconium coating with a thickness of ~2.5 μm was applied to the samples using vacuum-arc deposition. Deposition of coating was carried out on a VU-2MBS setup. After that, the samples were exposed to compression plasma flows (CPFs) generated by a magneto-plasma compressor of compact geometry [16]. The treatment was carried out with three plasma pulses generated in a residual nitrogen atmosphere. The distances between the cathode and the sample during treatment with plasma pulses were 16 cm and 10 cm, which, according to calorimetric measurements, corresponded to absorbed energy densities Q = 15 J/cm^2 and Q = 35 J/cm^2 per pulse. Then the irradiated samples were annealed at a temperature of 550°C in air for up to 15 h.

The phase composition of the samples was studied using X-ray diffraction analysis (XRD) on a Rigaku Ultima IV diffractometer using monochromatic copper radiation Cu$K_{\alpha 1}$ (λ = 0.154178 nm). The microstructure of the samples was studied by scanning electron microscopy (SEM) using a Carl Zeiss LEO1455VP scanning electron microscope. Microhardness measurements of surface layers were carried out using a Wilson Instruments MVD 402 microhardness tester according to the Vickers method. The load applied to the indenter was 25 g.

RESULTS AND DISCUSSION

The main phases in the X-ray analyzed layers of the studied alloys with zirconium coatings are Al and Zr in pure aluminum Al, Si, and Zr in Al-Si and Al-Si-Cu-Mg silumins (Fig. 1). In addition to the main phases, the composition of the Al-Si-Cu-Mg alloy also includes compounds Al_7Cu_4Ni, Mg_2Si, $Al_8Si_6Mg_3Fe$, and Al_5FeSi.

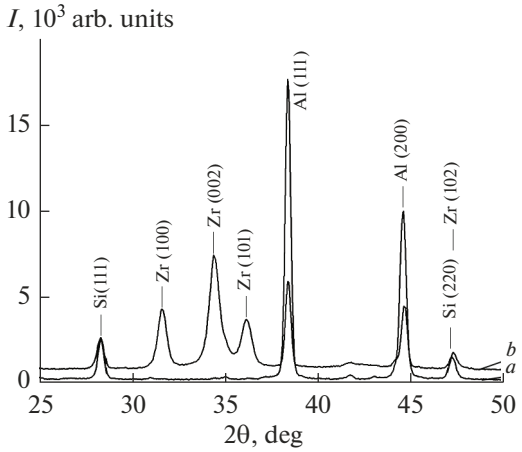

Fig. 1. X-ray diffraction pattern of Al-Si-Cu-Mg silumin samples (*a*) before and (*b*) after deposition of Zr coating.

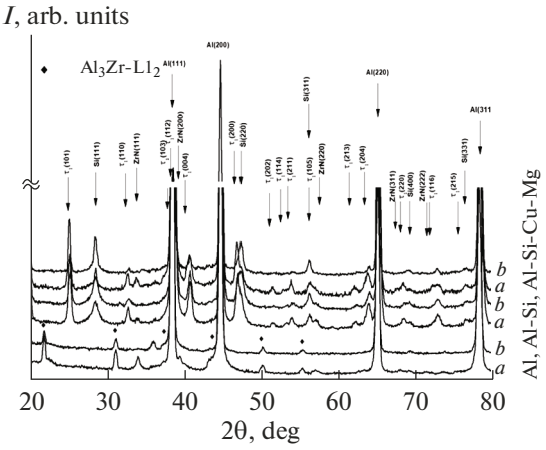

Fig. 2. Diffraction pattern of samples of alloys Al, Al-Si and Al-Si-Cu-Mg with zirconium coating treated with compression plasma flows at an absorbed energy density of (*a*) Q = 15 J/cm^2 and (*b*) Q = 35 J/cm^2.

Since under the influence of plasma pulses with an absorbed energy density of 15 J/cm^2 melting of the surface layer and liquid-phase mixing of the coating and substrate elements occur followed by crystallization under ultra-fast cooling conditions, then, as a result, the Al_3Zr phase with a cubic crystal lattice $L1_2$ (Fig. 2) and a lattice parameter a = 0.4071± 0.0006 nm is formed in the Zr–Al samples. An increase in the absorbed energy density to a value of 35 J/cm^2 leads to a decrease in the intensity of diffraction lines related to the Al_3Zr–$L1_2$ phase, which is most likely due to a

decrease in the zirconium concentration in the surface layer.

The presence of silicon in the composition of silumin samples causes the formation of the τ_1 phase with a tetragonal crystal lattice $D0_{22}$ in contrast to pure aluminum, where the formation of the Al_3Zr–$L1_2$ phase is observed under the same exposure conditions.

The metastable phase τ_1, which in various sources is designated as $(Al, Si)_3Zr$, $(Al_{1-x}Si_x)_3Zr$, or (Al, Si, Zr) [12–15], has a variable composition and lattice parameters depending on the crystallization conditions and composition of the alloy. In Zr–Al-Si samples treated with plasma at $Q = 15$ J/cm^2, the lattice parameters of the τ_1 phase are $a = 0.3890 \pm 0.0002$ nm and $c = 0.8806 \pm 0.0006$ nm. An increase in the absorbed energy density to 35 J/cm^2 leads to a decrease in the lattice parameters to $a = 0.3873 \pm 0002$ nm and $c = 0.8792 \pm 0.0006$ nm, which can be explained by an increase in the concentration of silicon in the τ_1 phase, the atomic radius of which is less than the atomic radius of aluminum ($r_{Si} = 132$ pm, $r_{Al} = 143$ pm). This does not exclude the influence of stresses that appear at high cooling rates.

In samples of the Al-Si-Cu-Mg alloy with a deposited Zr coating processed by CPF at $Q = 15$ J/cm^2, the lattice parameters of the τ_1 phase are equal to $a = 0.3892 \pm 0.0002$ nm and $c = 0.8812 \pm 0.0006$ nm, and at $Q = 35$ J/cm^2, they are equal to $a = 0.3871 \pm 0.0002$ nm and $c = 0.8813 \pm 0.0006$ nm. It can be seen that the presence of doping elements in this alloy (except silicon) leads to an increase in the lattice parameter c of phase τ_1 when exposed to a CPF with $Q = 35$ J/cm^2 as a result of the dissolution of intermetallic phases present in the initial structure of the alloy and the inclusion of additional elements in the crystal lattice of phase τ_1.

The use of nitrogen as a plasma-forming substance leads to the synthesis of nitrides in the near-surface layers of irradiated materials [16–18]. Thus, in all samples exposed to CPF with $Q = 15$ J/cm^2, zirconium nitride ZrN is formed. On samples treated with plasma at 35 J/cm^2, this phase could not be detected by X-ray diffraction, which is apparently due to a decrease in both the zirconium concentration in the surface layer and the nitrogen content at the residual atmosphere–surface interface with increasing Q [17]. In addition, diffraction peaks appear in the region $2\theta = 36°$, which can be attributed to aluminum nitride AlN with a hexagonal crystal structure.

The effect of CPF on the studied silumins also leads to a change in the lattice parameter of aluminum crystal. In samples of the Al-Si alloy with an applied zirconium coating, the aluminum lattice parameter decreases compared to the initial value from 0.4050 ± 0.0001 nm to 0.4045 ± 0.0001 nm at $Q = 15$ J/cm^2 and to 0.4043 ± 0.0001 nm at $Q = 35$ J/cm^2. This can be explained by the formation of a supersaturated substitutional solid solution Al(Si), the formation of which is also observed in other studies on irradiation of silumins with high-intensity energy flows [3, 7, 18], which, however, does not exclude the formation of Al(Si,Zr). After additional studies, it was found that the crystal lattice parameter in samples of the Al-Si alloy without a pre-deposited zirconium coating and exposed to CPF at $Q = 35$ J/cm^2 decreases compared to the initial value to 0.4045 ± 0.0001 nm; i.e., it is close in value to the results obtained in the system Zr–Al–Si 12.6 at % after irradiation by CPF.

The aluminum crystal lattice parameter for Zr–Al-Si-Cu-Mg samples exposed to CPF at $Q = 15$ J/cm^2 decreases from 0.4051 ± 0.0001 nm (in the initial sample) to 0.4045 ± 0.0001 nm owing to the formation of a supersaturated solid solution of aluminum with silicon. Upon irradiation by CPF with $Q = 35$ J/cm^2, the lattice parameter increases and amounts to 0.4051 ± 0.0001 nm, which correlates with the behavior of the lattice parameter c of phase τ_1. It is also necessary to take into account that the behavior of the lattice parameter in these samples can be influenced by the doping elements included in the alloy, in particular, magnesium, whose atomic radius is 1.6 Å and whose maximum solubility in aluminum is 18.9 at % [19]. In the Zr–Al samples, no changes in the lattice parameter were detected after exposure to the CPFs.

In silumin samples with a zirconium coating exposed to CPF, broadenings are visible at the bases of the silicon diffraction lines (Fig. 2). Decomposition of the experimentally obtained diffraction lines into Gaussian curves made it possible to establish that they represent a superposition of two lines, each of which refers to reflections from crystallographic planes of silicon (Fig. 3). It is known that the main contribution to the broadening of the diffraction line is made by dispersion of the structure and the presence of residual mechanical microstresses. The presence of a wide diffraction line (Fig. 3, line *2*) may indicate the presence of dispersed silicon crystals in the analyzed layer. In the initial structure of the alloys, the size of silicon inclusions ranged from a few (in the eutectic region) to tens of microns (primary inclusions).

An estimate of the size of the coherent scattering regions for silicon using this line by the Scherrer formula without taking into account possible microstresses showed that it is 6–7 nm. In studies on the effect of electron beams with energy density of 10–25 J/cm^2 on Al-Si-Cu-Mg silumin, it was found that the size of silicon inclusions decreases significantly [2]. The results of studies using transmission electron microscopy also established that the average size of silicon inclusions during such treatment is 180 nm, and in

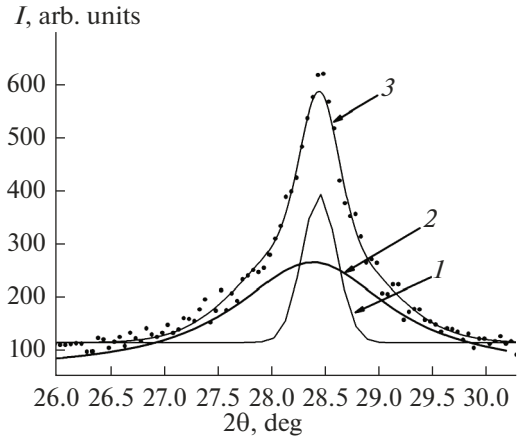

Fig. 3. Image of the diffraction line of silicon (111) after the mathematical decomposition of a sample of the Al-Si alloy with a zirconium coating after exposure to the CPF at Q = 35 J/cm^2 into components: (*1*) component of the diffraction line from coarse-crystalline silicon, (*2*) component of the diffraction line component from fine-crystalline silicon, and (*3*) the superposition of two diffraction lines. The dots indicate the experimental curve.

some cases, it is ~12 nm [2], which correlates with the results of these studies.

Using scanning electron microscopy, it was determined that, under the influence of CPF pulses, the synthesized Al_3Zr–$L1_2$ phase on the surface of aluminum samples with a zirconium coating has a dendritic structure with a dendrite size of 100–300 nm (Fig. 4a). The zirconium concentration for these samples is 2.6 at %, while the Zr content in Al-Si samples after exposure to CPF at the same absorbed energy density (Q = 35 J/cm^2) is 2.7 ± 0.1 at %; however, the volume fraction of fine inclusions of the τ_1 phase (Fig. 4b) is greater than that of Al_3Zr–$L1_2$ inclusions in aluminum samples. Apparently, this is due to the fact that, in pure aluminum samples, zirconium atoms are also present in the Al(Zr) solid solution while in silumin samples most of them participate in the formation of the τ_1 phase. The size of the synthesized inclusions of the τ_1 phase is 200–300 nm.

Studies on the treatment of Al-Si-Cu-Mg alloy with compression plasma flows revealed the formation of a cellular structure formed as a result of concentration supercooling of the melt [18]. The boundaries of cells were enriched in doping elements included in the alloy (Ni, Cu, Fe, and Mn). Irradiation of the Zr–Al-Si-Cu-Mg system by plasma flows led to the formation of a similar cellular structure with individual inclusions of the τ_1 phase (Fig. 4c). The concentration of zirconium in the samples was 1.4 ± 0.2 at %.

The analysis of the cross section of samples with zirconium coating showed that, as a result of plasma exposure, a doped layer is formed on their surface, the

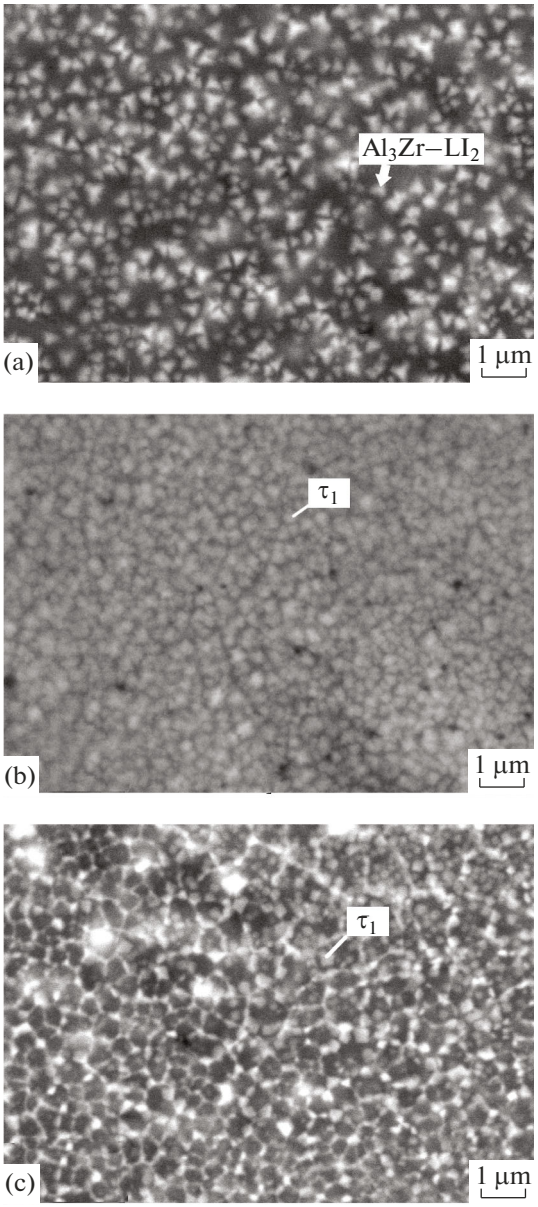

Fig. 4. Morphology of the surface of samples of alloys (a) Al, (b) Al-Si and (c) Al-Si-Cu-Mg with zirconium coating after exposure to CPF at Q = 35 J/cm^2.

thickness and composition of which is determined by the substrate material and processing modes (Fig. 5). The thickness of the doped layer in pure aluminum samples reaches 40 μm (Q = 15 J/cm^2); however, precipitates of the Al_3Zr–$L1_2$ phase are formed mainly in the near-surface layer up to 10 μm in thickness, and the underlying layer consists of a solid solution of Zr in Al. In samples exposed to CPF at Q = 35 J/cm^2, the volume fraction of synthesized Al_3Zr is significantly lower compared to the sample treated with a plasma flow at 15 J/cm^2. And this is due both to the greater depth of distribution of zirconium over the thickness

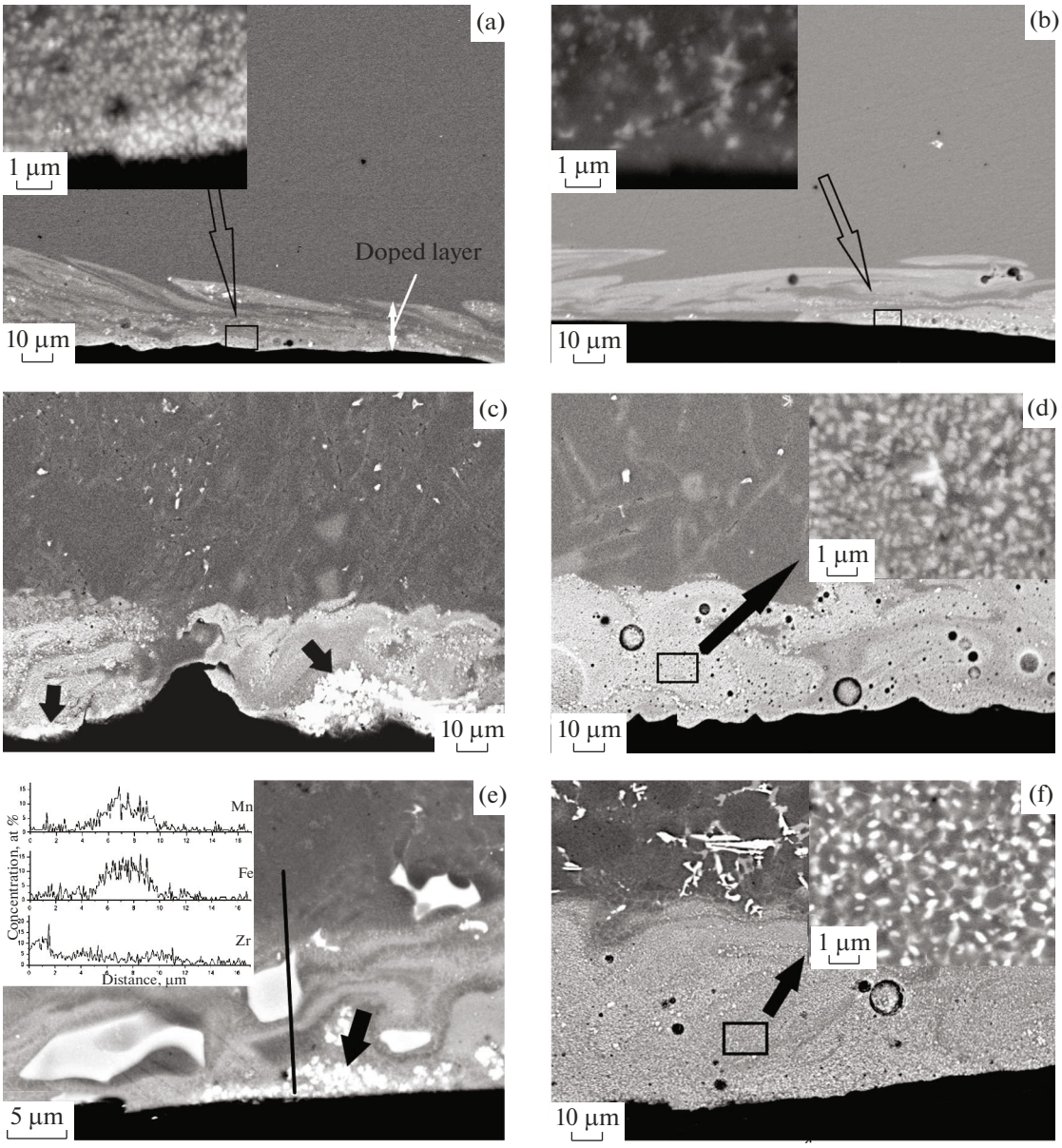

Fig. 5. Morphology of the cross sections of (a, b) Al_2 (c, d) Al-Si, and (e, f) Al-Si-Cu-Mg alloys with the layers of zirconium coating after exposure to CPFs at (a, c, e) $Q = 15$ J/cm^2 and (b, d, f) at $Q = 35$ J/cm^2.

of the near-surface layer and to the increase in the intensity of the process of erosion of the near-surface layer under plasma exposure. The size of the formed intermetallic inclusions, as on the surface, is 300 nm.

As a result of the effect of CPF on silumin samples, the thickness of the doped layer reaches 60 μm (Figs. 5d and 5f). Owing to the heterogeneity of the distribution of zirconium in the samples of silumins treated with CPF at $Q = 15$ J/cm^2, regions containing undissolved zirconium, areas of aluminum-based solid solution, and zones with fine inclusions of the τ_1 phase are formed in the volume of the modified layer. In the layer of the Al-Si-Cu-Mg alloy doped with Zr atoms by plasma treatment at $Q = 15$ J/cm^2, there are also unmelted intermetallic inclusions that were part of the original structure (Fig. 5e). An increase in the absorbed energy density of the CPF leads to an increase in the lifetime of the molten layer and the duration of convective flows [16]. As a consequence of this, the modified layer in samples processed at $Q = 35$ J/cm^2 is characterized by a more uniform distribution of zirconium throughout the thickness of the alloyed layer, since in this mode of exposure, complete dissolution of the initial intermetallic inclusions occurs, which leads to an increasing influence of the

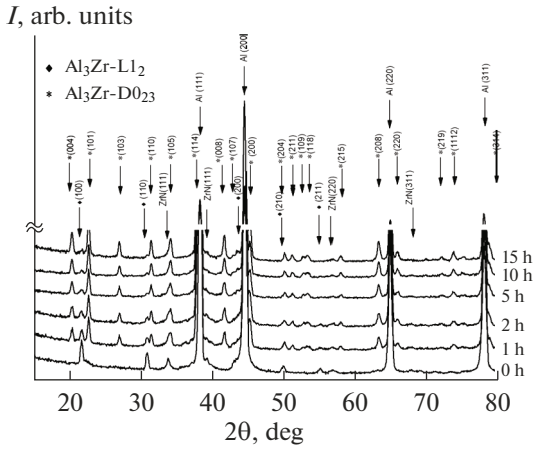

Fig. 6. X-ray diffraction pattern of zirconium-coated Al samples exposed to CPF at $Q = 15$ J/cm^2 before and after annealing at 550°C for various times.

doping elements of the alloy on the crystal lattice parameters of the aluminium and τ_1 phase.

In order to study the thermal stability of the Al_3Zr–$L1_2$ and τ_1 phases synthesized under the influence of CPFs, the samples were subjected to annealing at a temperature of 550°C. In a series of Zr–Al samples, a sample treated at 15 J/cm^2 was annealed since it contains a larger volume fraction of the formed Al_3Zr–$L1_2$ phase, and in the case of silumins, samples irradiated at 35 J/cm^2 and having a more uniform distribution of the doped element and accordingly the τ_1 phase over the doped layer were annealed.

For aluminum samples, annealing at 550°C for 30 min leads to partial decomposition of the Al_3Zr–$L1_2$ phase and the formation of a stable Al_3Zr compound with a $D0_{23}$ crystal structure. Figure 6 shows the kinetics of the process of normal polymorphic transformation of cubic Al_3Zr into a tetragonal structure upon annealing for 15 h.

After annealing at 550°C, needle-like structures are formed on the surface of the alloy (Fig. 7). On the basis of X-ray diffraction data, these precipitates can be attributed to the Al_3Zr–$D0_{23}$ compound. With increasing annealing time, the proportion of fine inclusions of the Al_3Zr–$L1_2$ phase decreases and the share of needle-shaped Al_3Zr–$D0_{23}$ precipitates increases. When the length reaches more than ~2 μm, the needle-like precipitates disintegrate into individual globular particles with lower surface energy.

Thus, as a result of annealing at 550°C for 30 min of the Zr–Al-Si alloy treated with CPF pulses at $Q =$

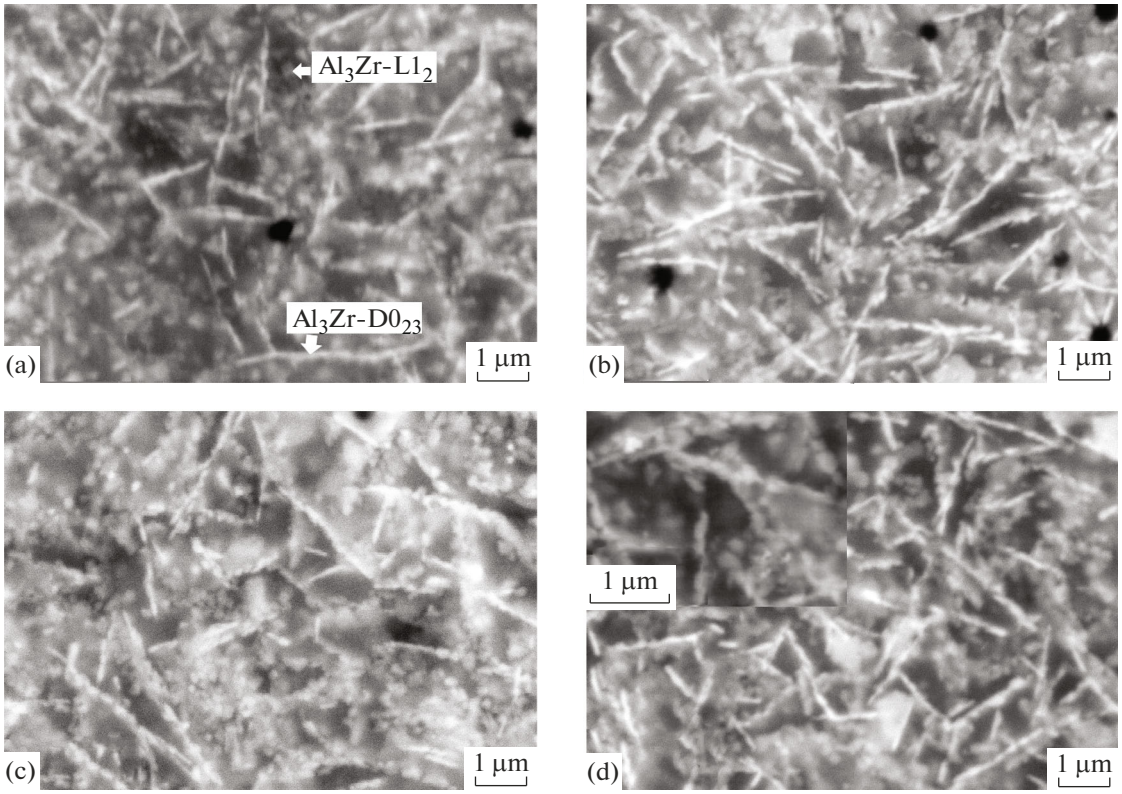

Fig. 7. Surface morphology of zirconium-coated Al samples exposed to CPF at $Q = 15$ J/cm^2 and subsequent annealing at 550°C for (a) 1 h, (b) 5 h, (c) 10 h, and (d) 15 h.

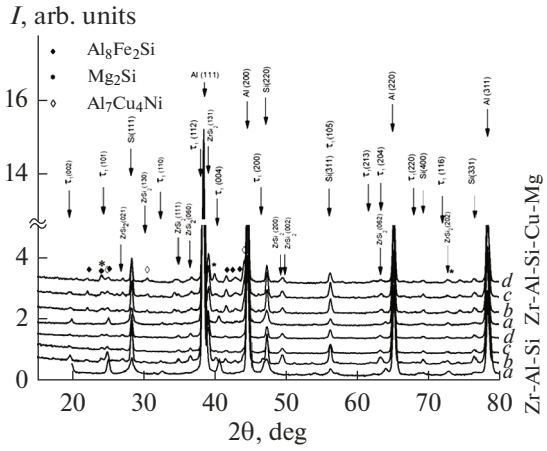

Fig. 8. Diffraction patterns of samples of alloys Al-Si and Al-Si-Cu-Mg with zirconium coating exposed to CPF at $Q = 35$ J/cm^2 (a) before and after annealing at 550°C for (b) 30 min, (c) 1 h, and (d) 2 h.

35 J/cm^2, the crystal lattice parameter c increases to values of 0.8943 nm, and the parameter a is 0.3872 nm (Fig. 8); this may indicate a decrease in the concentration of Si atoms in the crystal lattice of this phase. A further increase in the annealing time does not lead to such a significant change in the lattice parameters of the τ_1 phase.

Both a shift of the diffraction lines of aluminum to the region of smaller angles in the diffraction pattern of the annealed samples indicating the decomposition of a supersaturated solid solution based on aluminum and an increase in the intensity of the diffraction lines of silicon (Fig. 8) are observed. In this case, the component of the diffraction line from fine-crystalline silicon disappears, which indicates the process of coagulation of silicon precipitates occurring under the action of diffusion.

Increasing the annealing time of silumin samples to 2 h leads to the decomposition of the τ_1 phase and the formation of zirconium silicide $ZrSi_2$. Thus, when the Zr–aluminum and Zr–silumin systems are exposed to CPFs and subsequent annealing, phase transitions occur, which can be schematically represented as follows:

$$\mathrm{Zr + Al \rightarrow Al(Zr) + Al_3Zr - Ll_2}$$
$$\rightarrow \mathrm{Al + Al_3Zr - D0_{23}},$$
$$\mathrm{Zr + Al + Si \rightarrow Al(Si,Zr) + Si +}$$
$$\mathrm{\tau_1 - D0_{22} \rightarrow Al + Si + ZrSi_2}.$$

In samples of the Zr–Al-Si-Cu-Mg system subjected to CPFs and subsequent annealing at 550°C, phase changes similar to undoped silumin AK12 are observed: decomposition of the τ_1–$D0_{22}$ phase and the formation of the $ZrSi_2$ compound. At the same time, annealing of these samples leads to the formation of intermetallic compounds Al_7Cu_4Ni and Al_8Fe_2Si and Mg_2Si silicide. Data on energy-dispersive microanalysis confirmed that particles of the Mg_2Si phase coagulated under the action of diffusion are formed in the form of dendritic structures (Fig. 9). According to X-ray spectral analysis, the concentration of magnesium on the surface of these samples is 1.1 at %.

Using scanning electron microscopy, it was found that zirconium disilicide $ZrSi_2$ in samples of Zr–Al-Si and Zr–Al-Si-Cu-Mg exposed to CPF at $Q = 35$ J/cm^2 and annealed at 550°C is formed in the form of lamellar-like precipitates (Fig. 10). In addition, silicon crystals are clearly observed on the surface of Zr–AK12 samples etched in a NaOH solution with a concentration of 5 mol/L. In addition to $ZrSi_2$, areas of coagulation of doped elements included in the composition of the initial alloy are observed on the surface of the Al-Si-Cu-Mg alloy (Figs. 10c and 10d).

As a result of the structural-phase transformations that occurred in the modified layers of the materials under study, the microhardness is changed (Fig. 11). Thus, the microhardness of the initial Al alloy was $H_{v0} = 0.4$ GPa, and after irradiation with plasma pulses, the microhardness of the surface layer of Zr–Al increases to $H_v = 1.2$ GPa. The increase in microhardness can be influenced by solid solution and dispersion strengthening mechanisms. Annealing at

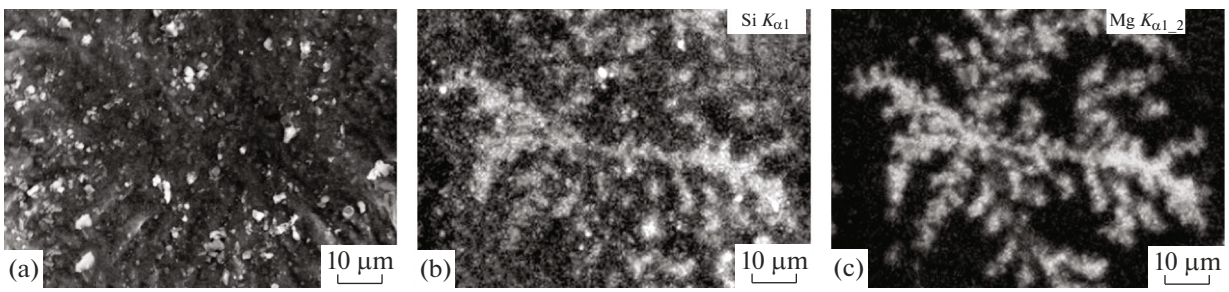

Fig. 9. Distribution of elements over the surface of a sample of the Al-Si-Cu-Mg alloy with a zirconium coating after exposure to CPF and annealing at 550°C for 2 h. (a) SEM image of the sample, (b) distribution of Si, (c) distribution of Mg.

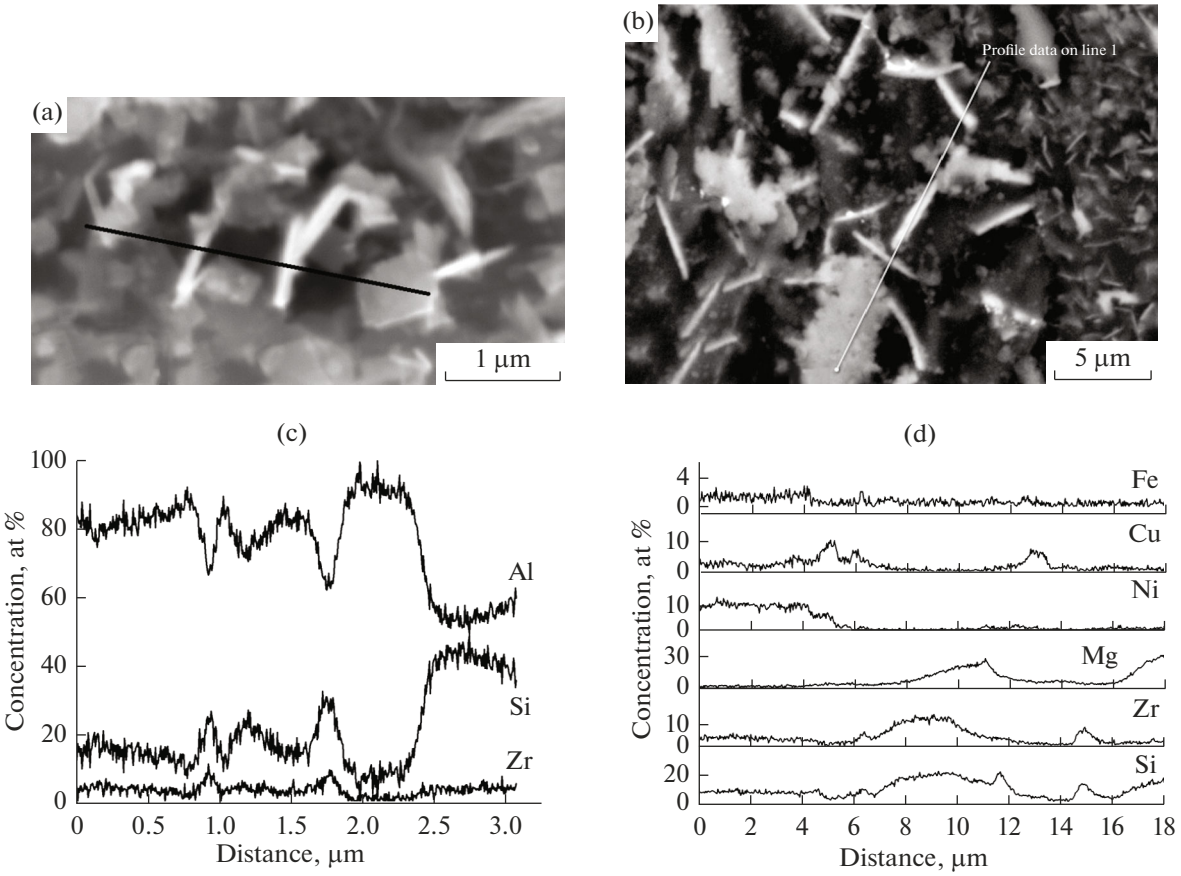

Fig. 10. (a, b) Surface morphology and (c, d) distribution of characteristic radiation of elements along line of samples of alloys Al-Si (a, c) and Al-Si-Cu-Mg (b, d) with zirconium coating exposed to CPF at $Q = 35$ J/cm^2 and subsequent annealing at 550°C for 2 h.

550°C for 15 h leads to its decrease owing to the processes of return and growth of grains. However, the microhardness of the near-surface doped layer after annealing remains higher than that of the initial structure by 67% ($H_v = 0.5$ GPa and $H_{v0} = 0.3$ GPa).

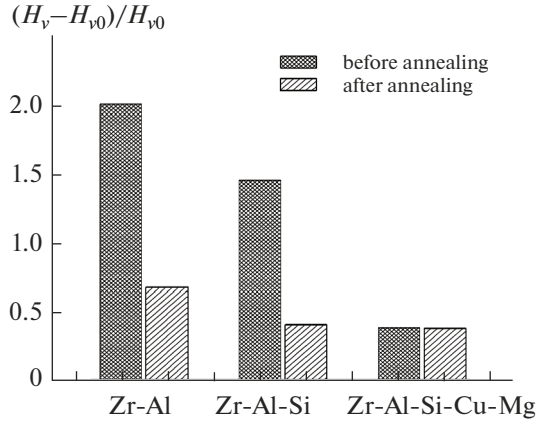

Fig. 11. Relative change in microhardness of Al, Al-Si, and Al-Si-Cu-Mg alloys exposed to CPF at 35 J/cm^2 before and after annealing.

For samples of the Al-Si alloy with applied coating and subsequent CPF treatment, an increase in microhardness from $H_{v0} = 0.6$ GPa to $H_v = 1.4$ GPa was observed. After annealing at 550°C for 2 h, the microhardness of the modified layer decreased and amounted to 0.7 GPa while for the initial sample annealed under the same conditions $H_v = 0.5$ GPa.

The least strengthening of the near-surface layer was observed for CPF-irradiated samples of Zr–Al-Si-Cu-Mg since the structure of the initial alloy already contains strengthening phases Al_7Cu_4Ni, Mg_2Si, and $Al_8Si_6Mg_3Fe$. The microhardness of the initial sample was 1.3 GPa, and the microhardness of the sample doped with zirconium atoms under the influence of CPF pulses was $H_v = 1.8$ GPa. After annealing at 550°C for 2 h, the microhardness of the irradiated samples was higher than the microhardness of the initial sample Al-Si-Cu-Mg subjected to annealing under the same conditions by ~38% ($H_{v0} = 0.8$ GPa and $H_v = 1.1$ GPa).

Thus, doping of silumin alloys Al-Si and Al-Si-Cu-Mg with zirconium atoms under the impact of CPFs makes it possible to increase the strength characteristics of the near-surface layer.

CONCLUSIONS

Thus, as a result of the studies, it was established that the effect of compression plasma flows with an absorbed energy density of the plasma flow of 15 J/cm^2 and 35 J/cm^2 on aluminum alloys Al, Al-Si, and Al-Si-Cu-Mg with a pre-deposited zirconium coating leads to the formation of a doped layer with a thickness of up to 60 μm with a metastable structural and phase state. In aluminum, precipitates of the Al_3Zr–$L1_2$ phase are formed in the form of finely dispersed inclusions with a size of 100–300 nm. In silumin alloys Al-Si and Al-Si-Cu-Mg, finely dispersed (200–300 nm) inclusions of the τ_1 phase with a crystalline structure of $D0_{22}$ are formed.

Annealing of samples at 550°C leads to the transformation of the Al_3Zr–$L1_2$ phase into Al_3Zr with a tetragonal structure $D0_{23}$ in aluminum samples and to the decomposition of the τ_1–$D0_{22}$ phase and the formation of $ZrSi_2$ in samples of silumin alloys. The resulting Al_3Zr–$D0_{23}$ phase in the form of needle-shaped precipitates up to 2 μm in length subsequently disintegrates into globular inclusions. The forming zirconium disilicide $ZrSi_2$ precipitates in the form of lamella-like inclusions.

The doped surface layer in alloys Al, Al-Si, and Al-Si-Cu-Mg has increased strength characteristics compared to the initial structure. The microhardness of the doped surface layer in the studied samples annealed at 550°C is higher than the microhardness of the initial annealed samples not subjected to doping by ~67% and ~40% for aluminum and silumin samples, respectively. Doping with zirconium atoms using CPFs increases the microhardness of the surface layer of aluminum by 3 times and the silumin alloys Al-Si and Al-Si-Cu-Mg by 2.3 and 1.4 times, respectively.

FUNDING

This work was supported by ongoing institutional funding. No additional grants to carry out or direct this particular research were obtained.

CONFLICT OF INTEREST

The authors of this work declare that they have no conflicts of interest.

REFERENCES

1. Belov, V.D., Piston silumins, *Vestn. Magnitogorsk. Gos. Tekh. Univ. im. G.I. Nosova*, 2005, no. 1 (9), pp. 32–34.
2. Laskovnev, A.P., Ivanov, Yu.F., and Petrikova, E.A., *Modifikatsiya struktury i svoistv evtekticheskogo silumina elektronno-ionno-plazmennoi obrabotkoi* (Modification of the Structure and Properties of the Eeutectic Silumin by Electron-Ion-Plasma Treatment), Minsk: Belaruskaya Navuka, 2013.
3. Hao, Y., Gao, B., Tu, G.F., Li, S.W., Dong, C., and Zhang, Z.G., Improved wear resistance of Al–15Si alloy with a high current pulsed electron beam treatment, *Nucl. Instrum. Methods Phys. Res., Sect. B*, 2011, vol. 269, no. 3, pp. 1499–1505. https://doi.org/10.1016/j.nimb.2011.04.010
4. Ivanov, Yu.F., Zaguliaev, D.V., Glezer, A.M., Gromov, V.E., Abaturova, A.A., Leonov, A.A., Semin, A.P., and Sundeev, R.V., Changes in surface structure and mechanical characteristics of Al–5wt%Si alloy after irradiation by electron beam, *Mater. Lett.,* 2020, vol. 275, p. 128105. https://doi.org/10.1016/j.matlet.2020.128105
5. Abbas, M.K. and Mahmoud, A.K., Laser surface treatment of Al–12%Si alloy, *Mater. Today: Proc.*, 2017, vol. 4, no. 9, pp. 9992–9996. https://doi.org/10.1016/j.matpr.2017.06.308
6. Zaguliaev, D.V., Ivanov, Yu.F., Klopotov, A.A., Ustinov, A.M., Shlyarov, V.V., and Yakupov, D.F., Evolution of strength properties and defect sub-structure of the hypoeutectic A319.0 alloy irradiated by a pulsed electron beam and fractured under tensile stress, *Materialia*, 2021, vol. 20, p. 101223. https://doi.org/10.1016/j.mtla.2021.101223
7. Bian, H., Aoyagi, K., Zhao, Y., Maeda, C., Mouri, T., and Chiba, A., Microstructure refinement for superior ductility of Al–Si alloy by electron beam melting, *Addit. Manuf.*, 2020, vol. 32, p. 100982. https://doi.org/10.1016/j.addma.2019.100982
8. Zakharov, V.V., About alloying of aluminum alloys with transition metals, *Met. Sci. Heat Treat.*, 2017, vol. 59, nos. 1–2, pp. 67–71. https://doi.org/10.1007/s11041-017-0104-2
9. Belov, N.A., Savchenko, S.V., and Hvan, A.V., *Fazovyi sostav i struktura siluminov: Spravochnoe izdanie* (Phase Composition and Structure of Silomines: Reference Book), Moscow: Mosk. Inst. Stali Splavov, 2001.
10. Mondolfo, L.F., *Aluminum Alloys: Structure and Properties*, Amsterdam: Elsevier, 1976.
11. Belov, N.A., Alabin, A.N., Matveeva, I.A., and Eskin, D.G., Effect of Zr additions and annealing temperature on electrical conductivity and hardness of rolled Al sheets, *Trans. Nonferrous Met. Soc. China*, 2015, vol. 25, pp. 2817–2826. https://doi.org/10.1016/S1003-6326(15)63907-3
12. Hirano, T., Ohtani, H., and Hasebe, M., Thermodynamic analysis of the Al–Si–Zr ternary system, *High Temp. Mater. Processes*, 2010, vol. 29, nos. 5–6, pp. 347–371. https://doi.org/10.1515/ HTMP.2010.29.5-6.347
13. Gao, T., Li, D., Wei, Z., and Liu, X., Evolution, microhardness of ZrAlSi intermetallic and its impact on the elevated-temperature properties in Al–Si alloys, *Mater. Sci. Eng., A*, 2012, vol. 552, pp. 523–529. https://doi.org/10.1016/j.msea.2012.05.081

14. Gao, T., Cui, X., Li, X., Li, H., and Liu, X., Morphological evolutions and growth patterns of Zr-containing phases in aluminum alloys, *Cryst. Eng. Commun.*, 2014, vol. 16, pp. 3548–3557. https://doi.org/10.1039/c3ce42548g
15. Guo, J.Q. and Ohtera, K., An intermediate phase appearing in Ll_2–Al_3Zr to D023–$A1_3Zr$ phase transformation of rapidly solidified Al–Zr alloys, *Mater. Lett.*, 1996, vol. 27, pp. 343–347.
16. Uglov, V.V., Cherenda, N.N., Anishchik, V.M., Astashinskii, V.M., and Kvasov, N.T., *Modifikatsiya materialov kompressionnymi plazmennymi potokami* (Modification of Materials by Compression Plasma Streams), Minsk: Belaruss. Gos. Univ., 2013.
17. Cherenda, N.N., Shimanskii, V. I., Uglov, V.V., Astashinskii, V.M., and Ukhov, V.A., Nitriding of steel and titanium surface layers under the action of compression plasma flows, *J. Surf. Invest.: X-Ray, Synchrotron Neutron Tech.*, 2012, vol. 6, no. 2, pp. 319–325. https://doi.org/10.1134/S1027451012040088
18. Cherenda, N.N., Bibik, N.V., Uglov, V.V., Astashinskii, V.M., and Kuz'mitskii, A.M., Modification of eutectic silumin surface layer by compression plasma flows, *Fiz. Khim. Obrab. Mater.,* 2012, no. 3, pp. 37–42.
19. *Diagrammy sostoyaniya dvoinykh metallicheskikh system: Spravochnik* (Phase Diagrams of Binary Metallic Systems: Handbook), Lyakishev, N.P., Ed., Moscow: Mashinostroenie, 1996, vol. 1.

Translated by S. Rostovtseva